Performance Enhancement of TBAI Capped CdSe-Quantum Dot Sensitized Solar Cells by an Interlayer Gold Nanoparticles

M. Nabil[a*], K. Easawi[b], T. Abdallah[c], S. Abdallah[d], M. K. Elmancy[e], S. Negm[f], H.Talaat[g]

[a,b,d,f]*Mathematical and Physical Engineering Department, Faculty of Engineering (Shoubra), Banha University, Cairo, Egypt*

[e]*Physics Department, Faculty of Science, Benha University*

[c,g]*Physics Department, Faculty of Science, Ain Shams University, , Cairo, Egypt*

[a]*Email: Mohammed_diab35@yahoo.com,* [b]*Email: dr_easawi@yahoo.com*

[c]*Email: Tamerabdallah74@gmail.com,* [d]*Email: dr.saiedabdallah@yahoo.com*

[e]*Email: m.r.mansy@gmail.com,* [f]*Email: drnegm@hotmail.com,* [g]*Email: hassantalaat@hotmail.com*

Abstract

The photovoltaic performance (PV) of quantum dot sensitized solar cells (QDSSCs) has been studied by the addition of gold nanoparticles (Au NPs) at three configuration interlayer positions in the photoanodes. The resulting photoanodes are (i) Fluorine doped tin oxide (FTO) /Au NPs/TiO_2/CdSe QDs,(ii) FTO/TiO_2/Au NPs/CdSe QDs and (iii) FTO/TiO_2/CdSe QDs/Au NPs. The TOPO and HDA capping of CdSe QDs has been modified to be TBAI in order to decrease the CdSe-TiO_2 molecular separation. The average size of Au NPs is ~ 15nm as measured by HRTEM. Our results show that the configuration with Au NPs deposited directly on FTO exhibit a noticeable improvement of the power conversion efficiency (*PCE*) from 0.62% to 1.1%, while the other two configurations show a slight improvement in their performance. The effect of Au NPs in the three photonode configurations on the photovoltaic performance are discussed.

Keywords: Quantum dot sensitized solar cell (QDSSCs); gold NPs; Plasmon; TBAI; capping exchange.

----

* Corresponding author.

1. Introduction

Recently, a great effort has been done by researchers to improve the performance of the various solar cell types that belong to the third generation, especially quantum dots sensitized solar cells (QDSSCs) [1,2]. In these QDSSC, quantum dots (QDs) are adsorbed onto large band gap metal oxides such as TiO_2 to act as light harvesting sensitizers [3,4]. These QDs posses many attractive properties such as the ability to tune their band gaps, high extinction coefficients due to quantum confinement , large intrinsic dipole moment leading to rapid charge separation and as well low manufacturing cost [5]. Among the different QD_S semiconductor sensitizers such as (CdS, CdSe, PbS, InP, etc,) for QDSSCs, CdSe QDs were intensively studied due to it is band gap matching for solar light absorption along with wide range of band gap tenability and high extinction coefficient [6-8]. Usually, colloidal CdSe QDs prepared by hot injection methods are enclosed within a shell from organic ligands such as tri-n-octylphosphine oxide (TOPO), oleic acid (OA), and hexadecylamine (HDA) [9]. These organic ligands represents a barrier against charge transfer from the CdSe QDs which in turn decrease the electronic coupling between QDs and TiO_2 and increase the interface resistance to the charge carriers flux [10]. CdSe with inorganic ligands as tetrabutylammonium iodide (TBAI) have a shorter chain can exhibit smaller size and higher electron mobility [11]. Thereby, the diffusion path of photoelectrons from CdSe QDs is reduced and the electronic coupling with TiO_2 could be enhanced by the decrease of interface resistance. Hence, an overall enhancement in performance of CdSe-QDSSCs is expected to be achieved as a result of better photoelectron collection efficiency [12]. On the other hand, a lot of efforts currently are running to improve the photovoltaic performance of QDSSCs by insertion of an interfacial layer of plasmonic metal NPs in order to improve its electrical and optical properties [13]. Among the different plasmonic metal NPs, gold (Au) NPs interlayer's have showes high potential in enhancing the performance of QDSSCs due to their outstanding optical properties. Kouskoussa and his colleagues studied the effect of ultrathin metal layer insertion between conducting FTO and ZnO layer in organic photovoltaic [14,15]. An interfacial Au NPs layer between the FTO substrate and the TiO_2 mesoporous layer in CdS-QDSSC was studied by Guang Zhu and his colleagues and the *PCE* has been increased from 0.86% to 1.62% upon Au NPs layer insertion [16]. M. Oliveira and his colleagues employed the plasmon-induced photoelectron-chemistry from gold NPs placed in two different configuration in dye-sensitized solar cells (DSSCs), TiO_2/Au NPs/Dye and TiO_2/Dye/Au NPs, to improve the photovoltaic performance of the fabricated DSSC devices through increasing light scattering and hot-electrons utilization [17]. In this work we report on systematic study employing Au NPs layer at three configurations and the resulting difference in *PCE* due to their different configurational positions. We study here three different interfacial configuration of Au NPs layers in surface modified TBAI capped CdSe QDs in QDSSCs, the three configuration are (i) Au NPs as interfacial layer between FTO and TiO_2 (FTO /Au NPs /TiO_2 /CdSe QDs) (ii) Au NPs placed on top of the TiO_2 mesoporous film (FTO/TiO_2/Au NPs/CdSe QDs) and (iii) Au NPs placed on top of the active layer CdSe QDs (FTO/TiO_2/CdSe QDs/Au NPs).

2. Experimental details

2.1. Materials

 FTO substrate with sheet resistance12 Ω square-1 (TEC-15, Sigma-Aldrich) used for both photoanode and

counter electrodes. Cadmium oxide (CdO), TOPO, Selenium (Se), HDA, Hydrogen tetrachloroaurate(III) trihydrate ($HAuCl_4.3H_2O$), Zinic nitrate ($Zn(NO_3)_2$) and Tetrabutylammonium iodide (TBAI) were obtained from Sigma-Aldrich. Trioctyiphosphine (TOP) was purchased from Fluka. Trisodium citrate dehydrate ($Na_3C_6H_5O_7.2H_2O$), sodium borohydride ($NaBH_4$) and Ascorbic acid , Cetyltrimethylammonium bromide (CTAB), Cupric acetate monohydrate ($Cu(OAc)_2.H_2O$) elemental sulfur (S) and sodium sulfide nonahydrate ($Na_2S \cdot 9H_2O$) were reagent grade and used as received without further purification.

2.2. Synthesis of CdSe QDs nanopaticles with TBAI capping

CdSe QDs were prepared according organometallic method [18]. Cd precursor is prepared from 0.3 g (2.34 mmol) of CdO in 2 g (0.701 mol) oleic acid at $170^{o}C$. A mixture of 2 g (4.77 mmol) of TOPO and 2g (8 mmol) of HDA are added to the solution and held at $180^{o}C$ for nearly 5 min. Meanwhile, Selenium precursor by dissolving a 0.3 g (3.79 mmol) of selenium in 4 mL (8.8 mmol) of TOP. The Cadmium solution is loaded to a tri-neck flask and heated to $130^{o}C$ followed by the injection of the selenium solution drop wise to the reaction mixture and heating to $220 \ ^{o}C$ for 15 min, during this time CdSe QDs indicated by the change in color in the reaction mixture. The heating is tuned off to allow cooling of the three-neck flask to $100°C$, and left at this temperature for 5 minutes. At this point the reaction was quenched by rapidly cooling the solution in a water bath. CdSe NCs are washed via dispersion in hexane and ethanol followed by centrifugation.

To obtain the TBAI coated nanocrystals, CdSe nanocrystals (about 50mg/ml) coated with TOPO, HDA and Oliec acid was put in 37mg/ml of TBAI dissolved in IPA and heated at $70^{0}C$ for 24hours until the nanocrystals were totally dispersed in TBAI to get a clear solution. A copious amount of hexanes was added to precipitate the nanocrystals, and the NPs were collected by using centrifugation. After two repetitions of dissolution/precipitation with TBAI/hexanes, the surface capping ligands were replaced by TBAI.

2.3. Synthesis of gold nanoparticles

Aqueous solution from Au NPs was prepared following the method previously reported by Z. Sun group **[19]**. Briefly, 2.5 mL of a $HAuCl_4 \cdot 3H_2O$ solution (0.2% w/v) in 50 mL of water was brought to boil and then 2 mL of $Na_3C_6H_5O_7 \cdot 2H_2O$ (1% w/v) was suddenly added under vigorous stirring. The solution was kept boiling until the color of the solution change to red and then let to cool until room temperature was reached. The final concentration of Au NPs was adjusted to 10µL of 20% of Au NPs by adding distilled water and was used for the QDSSC devices fabrication.

2.4. Fabrication of photoanodes

The solar cell photoanode is prepared on FTO coated glass (sheet resistance12Ω square^{-1}, Solaronix) that was first ultrasonically cleaned using detergent solution, water, and acetone respectively. In the beginning, A compact TiO_2 layer was deposited on the FTO by spin coating 100 *μl* of 0.1 M isopropanol solution of Titanium Isopropoxide (TIP) at 1000 rpm for 10 seconds. The coating cycle was repeated twice and the substrate was annealed at 500 ℃ for 1 hour. The layer of TiO_2 P25 mesoporous of 10.58±0.2 µm thickness was coated over the blocking layer (BL) by the doctor blade technique and sintered at 500 ℃ for 1 h. The coating paste was

prepared by mixing TiO_2 P25 and ethyl cellulose as a binder in terpineol [20]. The obtained TiO_2 mesoporous film were then coated with QDs sensitizers by drop casting of TBAI-QD aqueous dispersion with (30mg/ml) and staying for 1 h before being rinsed sequentially with water and ethanol. All the photoanodes were passivated by two SILAR cycles of ZnS as reported elsewhere.

Three different QDSSC configurations containing Au NPs layer were assembled and a schematic representation of the devices is depicted in Figure 1. 10 μ L of 20% of Au NPs solution dispersion was drop-casted (i) on top of FTO glass (FTO/Au NPs/TiO_2/TBAI-CdSe QDs), (ii) on top of the TiO_2 mesoporous film (FTO/TiO_2/Au NPs/TBAI-CdSe QDs) and (iii) on top of the TBAI-CdSe QDs (FTO/TiO_2/TBAI-CdSe QDs/Au NPs).

2.5. QDSSC devices fabrication

The QDSSCs devices were fabricated by assembling the photoanodes and the prepared counter electrodes (CEs) by using parafilm as a spacer between the two electrodes. The CE of CuS was deposited on other FTO by a SILAR method [21].A regenerative polysulfide electrolyte (S^{2-}/S_x^{2-}) made out of 1M Na_2S, 1M S, and 0.1M KCl in distilled water was utilized to fill the space between the two terminals electrodes [21].
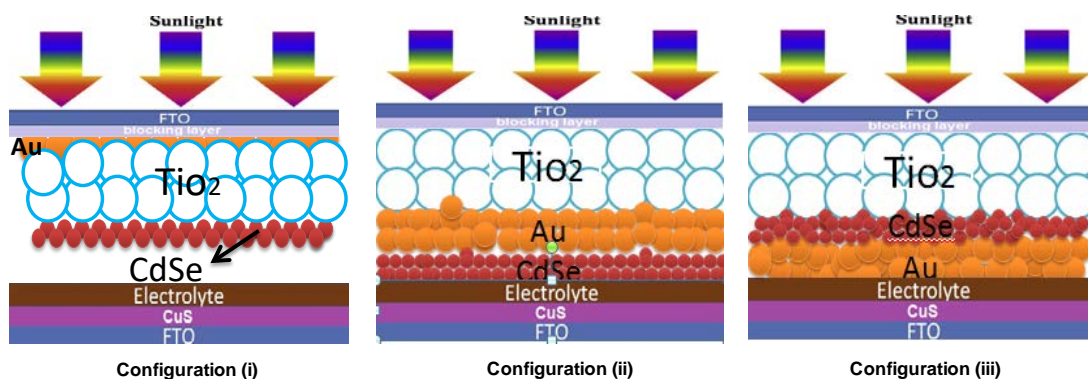

Figure 1: A schematic representation show the three different configurations of Au NPs layer into the assembled QDSSC devices.

2.6. Characterizations and measurements

The UV-Vis absorption spectra of CdSe QDs were recorded using (Jasco 670 with 1cm quartz cuvettes) spectrophotometer. The size and morphology was determined using high resolution transmission electron microscopy (HRTEM, JEOL JEM-2100 operated at 200KV with high resolution Gatan CCD bottom camera, Orius SC200). Photovoltaic solar cell measurements were performed using a solar simulator device (San-Ei Electric XES-40S1) at AM 1.5 with 1 sun illumination intensity (100 mW/cm^2), and current density–voltage (J–V) data were recorded using a source meter unit (Keithley SMU 2400).

3. Results and discussion

3.1. Structural and Morphology Analysis

The UV-vis absorption spectrum of TOPO, HDA capped CdSe QDs and TBAI capped CdSe QDs are shown in Figure 2. From the spectra, it is observed that the absorption peak shifts from 584 nm for the TOPO and HDA capped CdSe QDs to 576 nm for the TBAI capped CdSe QDs. Also the TBAI capped CdSe quantum dots in ethanol show a higher absorption than TOPO, HDA capped CdSe QDs in Toluene due to their different solubility behaviors.
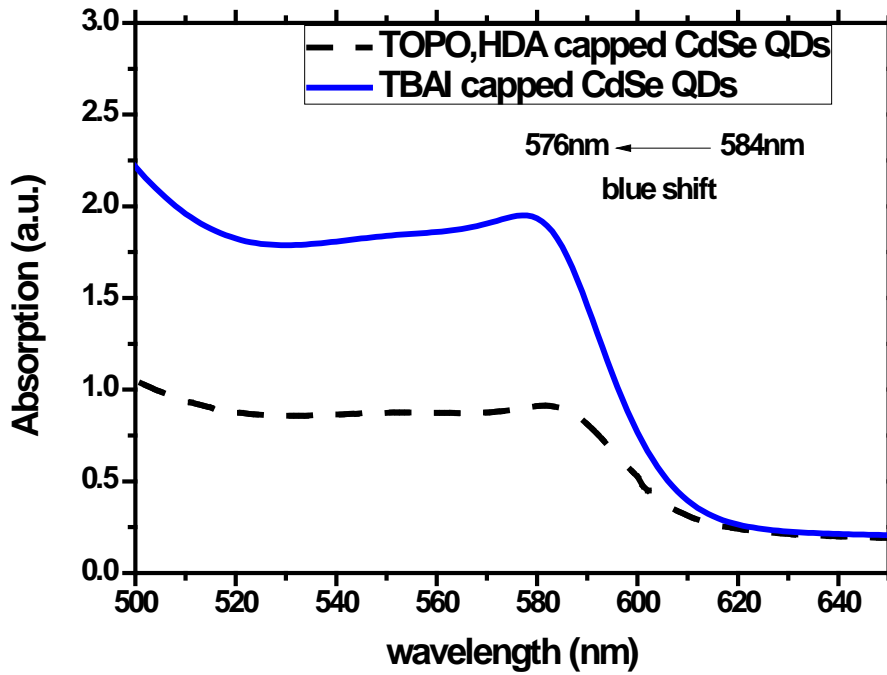

Figure 2: Absorption spectra of TOPO and HDA capped CdSe QDs (dotted line) and TBAI capped CdSe QDs (solid line).

The nanoparticles size was estimated from the UV-Vis absorption spectra peaks using three methods. The first method is the Polynomial Fitting Functions (*PFF*) given by [22]:

$$D = (1.6122 \times 10^{-9})\lambda^4 - (2.657 \times 10^{-6})\lambda^3 + (1.6242 \times 10^{-3})\lambda^2 - (0.4277)\lambda + (41.57) \qquad (1)$$

where D(nm) is the size of a given CdSe QDs sample and λ_{max} (nm) is the wavelength of the optical excitonic peak of the corresponding sample. The second method is a simple exponential function proposed by Bacherikov and his co-workers [23].

$$S = 0.344 \exp\left(\frac{\lambda_{max} - 252.7}{129.3}\right) \qquad (2)$$

where S(nm) is the average diameter of particle size. λ_{max} (nm) is the wavelength of the optical first excitonic absorption peak. The third method is Effective Mass Approximation model (*EMA*) [24]. The band gap size is depend on the radius (*R*) of quantum dots which based on equation (2).

$$E_{gn} = E_{gb} + \frac{h^2}{8R^2}\left[\frac{1}{m_e} + \frac{1}{m_h}\right] - \frac{1.8e^2}{4\pi\varepsilon\varepsilon_0 R} \qquad (3)$$

where, E_{gn} is the electronic band gap for CdSe nanocrystals, E_{gb} is the band gap of bulk CdSe (1.74 ev), R is the average radius of nanoparticles. m_e is the electron effective mass (0.13 m_o), m_h is the hole effective mass (0.45 m_o) and ε is the dielectric constant for CdSe QDs [25]. The calculated CdSe crystalline sizes according to the three methods are tabulated in the Table (1), noting that (Bohr diameter of CdSe QDs is about 6nm).
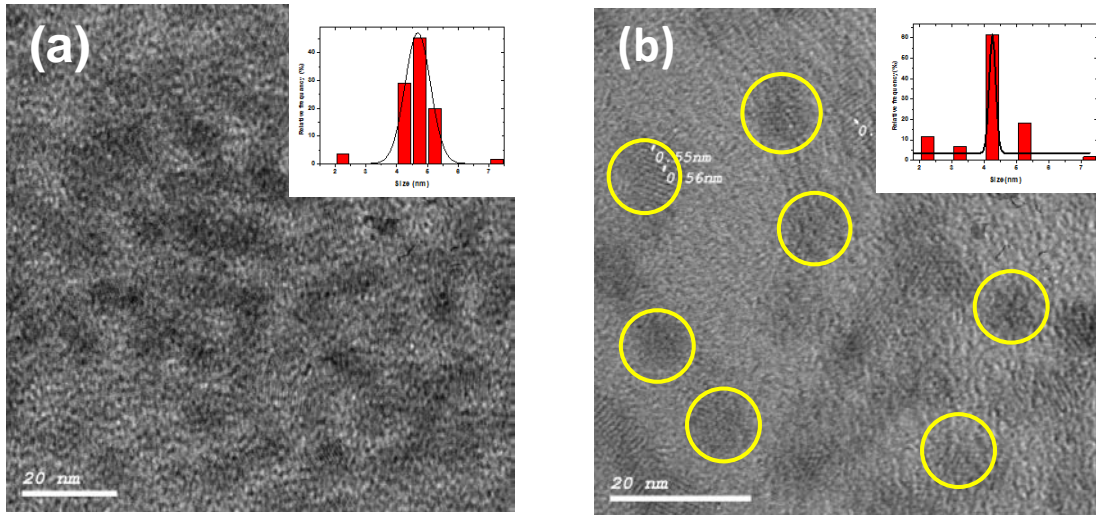

Figure 3: HRTEM images of CdSe nanocrystals (a) capped with TOPO & HDA, and (b) capped with TBAI. The inset of each micrograph is the histogram of particle size distribution.

The size of the nanoparticles in this study was also measured using TEM analysis as shown in Figure 3. It is clearly observed that the TBAI capped CdSe QDs Figure 3(b) are smaller in size than the TOPO, HDA capped counterparts shown in Figure 3(a) as it is also observed in Table 1. The reduction in size is a result of decreased surfactant length from 1.1nm for TOPO and HDA to 0.78nm for TBAI [26]. The decrease in the nanocrystals size during the capping exchange process may be due to the loss of Cd and Se atoms from the NPs surface as reported in other studies [27].

Table 1: The calculated size of TOPO, HDA capped CdSe QDs and TBAI capped CdSe QDs by first, second and third method using UV-vis absorption and also observed by HRTEM.

CdSe QDs Samples	First method (nm)	Second method (nm)	Third method (nm)	HRTEM (nm)
Capped with TOPO&HDA	4.02	4.49	4.72	4.72
Capped with TBAI	3.73	4.23	4.13	4.25

The difference of employing TOPO, HDA and TBAI as capping surfactant on CdSe QDs in the energy band gap is studied using Tauc's equation [28].

$$\alpha h \upsilon = A(h\upsilon - E_g)^n \tag{4}$$

where A is constant, α is the optical absorption coefficient, $h\upsilon$ is the energy of the incident photons, h is Planck's constant and n value depends on being either direct or indirect optical transition. In case of CdSe QDs, the transition is direct allowed semiconductor and n value is chosen to be 2 [29]. Hence, the energy gap (E_g) of CdSe QDs can be determined from the extrapolation of the linear part of the $(\alpha h\upsilon)^2$ versus $(h\upsilon)$ plot to the x-axis, as indicated in Figure 4. The resultant value of (E_g) for TBAI capped CdSe QDs with is found to be (2.07ev), while E_g for TOPO, HDA capped CdSe QDs with is found to be (2.05ev).
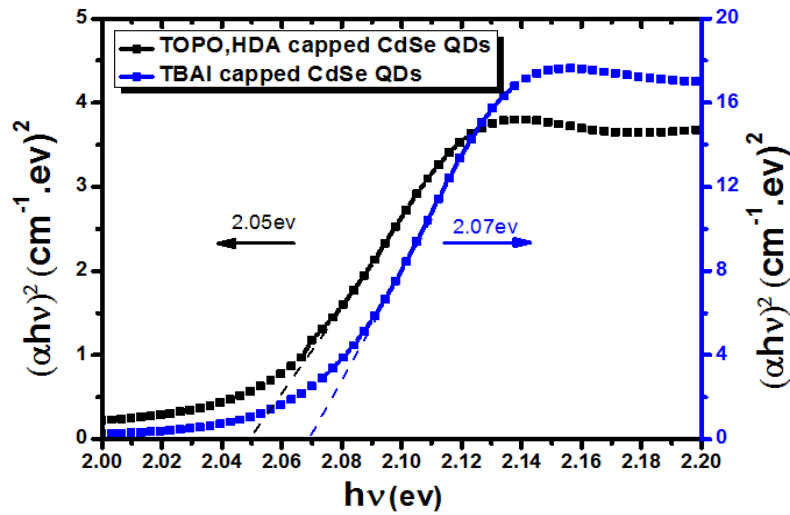

Figure 4: Tauc's plot for TOPO, HDA capped CdSe QDs and TBAI capped CdSe QDs.

The energy variation of the conduction band (CB) and valance band (VB) for CdSe QDs before and after surface modification with TBAI is shown by the following equations [30].

$$E_{cb} = E_{cb,bulk} + (E_{g,observed} - E_{g,bulk})(\frac{m_h}{m_h + m_e}) \tag{5}$$

$$E_{vb} = E_{cb} - E_{g,observed} \tag{6}$$

where $E_{g,bulk}$ is the CdSe bulk bandgap (1.74 eV) and $E_{cb,bulk}$ is the bulk conduction band minimum versus vacuum. $E_{g,observed}$ is the observed band gap which determined from the first absorption wavelength. The value of the E_{CB} of bulk CdSe ($\sim$ -4.3 eV vs. vacuum) as deduced from electron affinity is very close to the E_{CB} of TiO_2

($\sim$ -4.3 eV vs. vacuum) [30].

3.2. Photocurrent-Voltage Characterization

The photocurrent-voltage (J–V) curves of solar cells under solar irradiation for TOPO, HDA capped CdSe QDs (cell A) and TBAI capped CdSe QDs (cell B) are shown in Figure 5. The inset of Figure 5 are the image for photoanode of the (cell A) and (cell B). The photovoltaic parameter open circuit potential (V_{OC}), short-circuit current density (J_{SC}), fill factor (FF), and the total power conversion efficiency PCE of the (cell A) and (cell B) are given in Table 2.
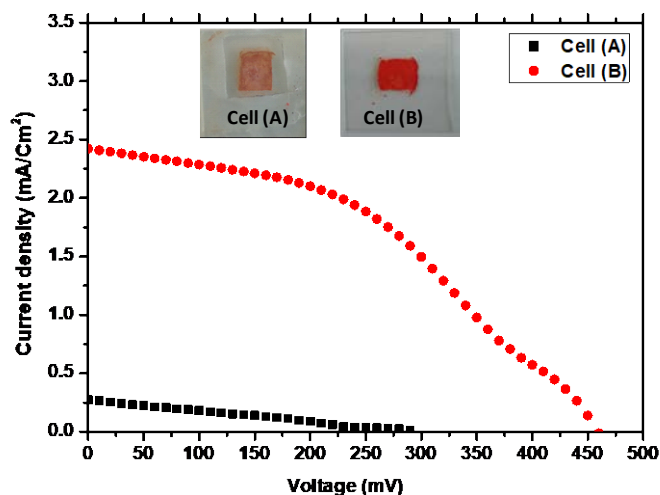

Figure 5: Photocurrent density–voltage curves of QDSSCs assembled with TOPO, HDA capped CdSe QDs and TBAI capped CdSe QDs. The inset is photographs for both photoanodes.

It is clear that, the performance of (cell B) is much better than that of (cell A). The increase efficiency of cell B (0.62%) is 10 times higher than that of cell A (0.07%). The larger efficiency of (cell B) is attributed to; (i) more diffusion of TBAI capped CdSe particles on TiO$_2$ film as shown in the inset of Figure 5.

Since for equal weight of the modified surface with TBAI capped CdSe QDs and the TOPO, HDA capped CdSe QDs, the TBAI capped CdSe QDs is allow more participating CdSe QDs on TiO$_2$ than TOPO , HDA capped CdSe QDs. (ii)The absorption band of TBAI capped CdSe QDs shifts to words solar band. (iii) The increase in photocurrent of cell (B) than cell (A) is due to the shift upward the E$_{CB}$ of TBAI capped CdSe QDs with less negative potentials (-4.277ev) (against vacuum) than E$_{CB}$ of TOPO, HDA capped CdSe QDs (-4.298ev), which increases the driving force for charge injection [31].

As shown in Table 2, the QDSSCs fabricated with TBAI capped CdSe nanoparticles exhibited better performance than the TOPO, HDA capped CdSe nanoparticles; where J_{SC} increased from 0.3 mA/Cm^2 to 2.4 mA/Cm^2, V_{OC} increased from 302 mV to 460 mV, and *PCE* increased from 0.07 % to 0.62 %.

Table 2: Photovoltaic parameters for TOPO, HDA capped CdSe QDs and TBAI capped CdSe QDs.

Sample	Ligand	J_{SC} (mA/cm^2)	V_{OC} (mV)	FF (%)	PCE (%)
Cell (A)	TOPO , HDA	0.3	302	38%	0.07
Cell (B)	TBAI	2.4	460	44%	0.62

Basically, employing TBAI as ligand for CdSe QDs plays two essential roles for improving the performance of QDSSCs. Firstly; TBAI passivated the localized surface states on the CdSe QDs surface which suppress the surface recombination loss of the photoelectrons. Secondly; TBAI ligand decreases the charge transfer resistance at the interface between CdSe QDs and TiO$_2$ that is in turn positively reflect on the photoelectrons injection efficiency at the interface. It is worth to mention that, TBAI passivation for CdSe QDs can also reduce the surface reactivity of CdSe QDs against the corrosive effect polysulfide electrolyte which enhances the QDSSC device stability.

3.3. The effect of Au NPs interfacial location on Photocurrent-Voltage for TBAI capped CdSe QDSSCs in the three configurations

The HRTEM images of the synthesized Au NPs are shown in Figure 6(a). The Au NPs were quasi-spherical structure with a diameter $\approx$ 15 nm. The UV-vis measurement was performed on a clear colloidal solution of Au NPs and the acquired spectrum is shown in Figure 6(b). The inset of Figure 6(b) shows a photograph of the Au NPs colloidal solution which has wine red color. The clear and sharp peak easily seen around 525 nm in the UV-vis spectrum is attributed to the surface plasmon absorption of the Au NPs.
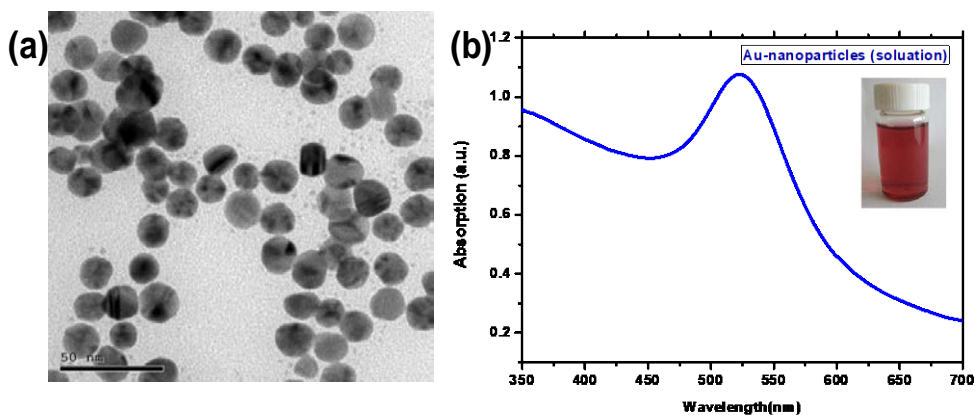

Figure 6: (a) HRTEM images of the gold nanocrystals, (b) UV–Vis absorption spectrum of the gold NPs. The photograph of the gold NPs aqueous solution shown in the inset of (b).

The HRTEM image of Au NPs dispersed in TiO_2, in the second configuration (FTO/TiO_2 NPs/Au NPs) are shown in Figure 7(a). It is observed that Au NPs were scattered randomly within the larger TiO_2 particles (about 20–25 nm). The UV-vis absorption spectra for FTO/TiO_2/Au NPs are shown in Figure 7(b) reveals that, the peak at 525 nm of Au NPs was superimposed on the spectrum of bare FTO/TiO_2. This attained result indicates the successful incorporation between the Au NPs and TiO_2 in the photoelectrode.
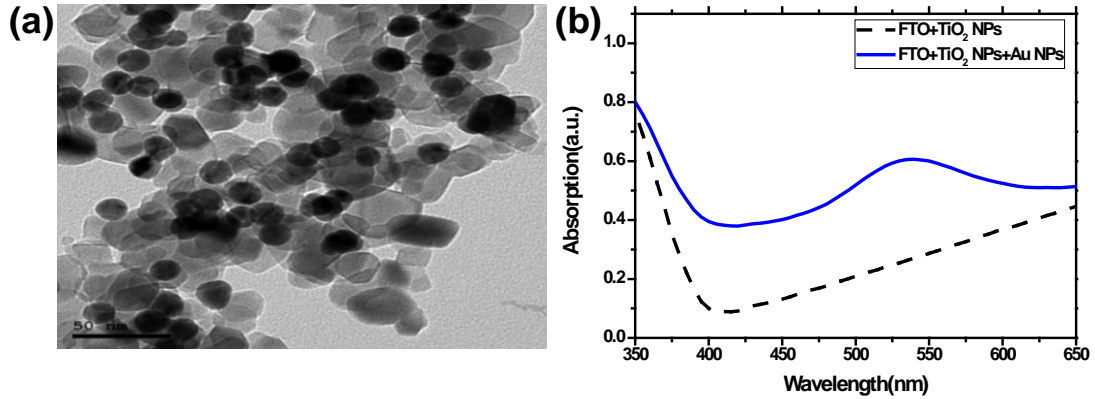

Figure 7: (a) HRTEM image of TiO_2 NPs decorated with Au NPs, (b) UV-visible absorption spectra of TiO_2 NPs on FTO substrate (dashed line) and TiO_2/Au NPs on FTO substrate (solid line).

The HRTEM of the TiO_2 NPs/CdSe after Au NPs decoration in the third configuration (FTO/TiO_2/CdSe QDs/Au NPs) is shown in Figure 8(a). The optical transmittance spectra of these layer configuration TiO_2 NPs /CdSe after Au NPs deposition are shown in Figure 8(b), with an absorption that is a combination of the surface Plasmon Au NPs and CdSe QDs.
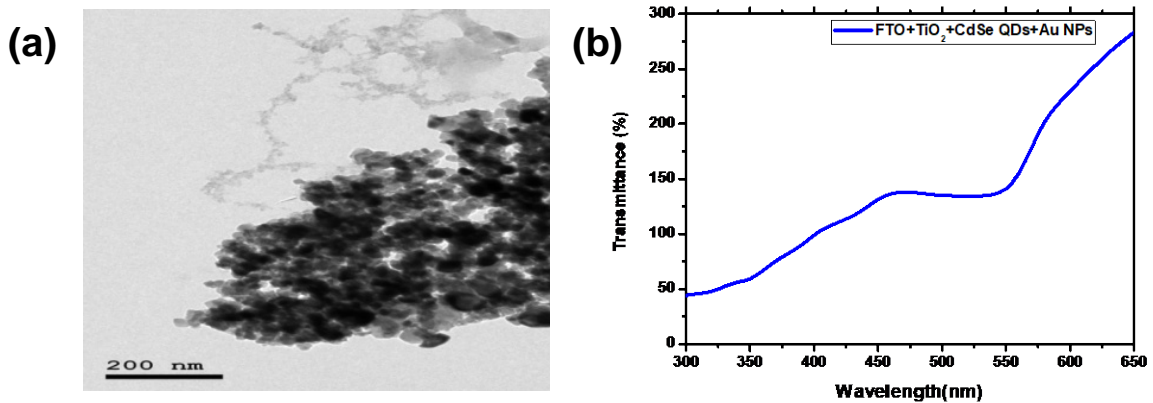

Figure 8: HRTEM image of TiO_2/CdSe QDs/Au nanoparticles. (b) Transmittance spectra of TiO_2/CdSe QDs/Au nanoparticles.

The (J–V) curves of the three different configurations of the fabricated solar cells with Au NPs and without Au NPs are shown in Figure 9. The observed (V_{oc}), (J_{sc}), (FF) and PCE are listed in Table 3. It is observed that, enhancements in the overall photovoltaic performance for all assembled devices were achieved by the

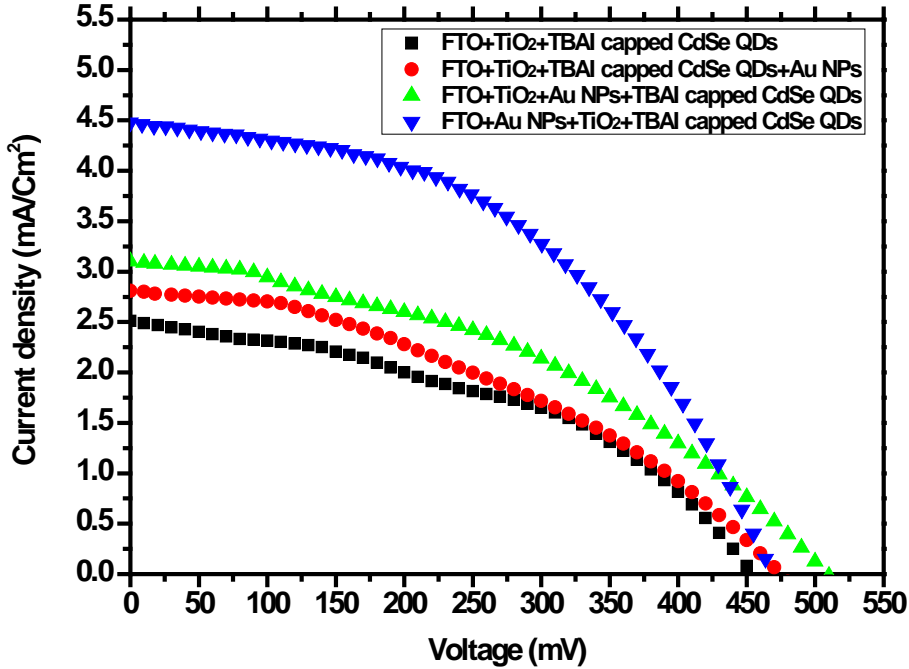employment of Au NPs. The energy levels of FTO, Au, TiO$_2$ and CdSe QDs are schematically shown in Figure 10.

Figure 9: Photocurrent density–voltage curves of all fabricated CdSe QDSSC.

Table 3: Parameters obtained from the *J–V* curves of Au NPs decorated on photoanodes for CdSe QDSSCs.

Configuration of solar cells	J_{SC} (mA/cm^2)	V_{OC} (mV)	*FF* (%)	*PCE* (%)
FTO+TiO$_2$+CdSe QDs	2.4	460	44	0.62
FTO/Au NPs/TiO$_2$/CdSe QDs	4.4	476	47	1.1
FTO/TiO$_2$/Au NPs/CdSe QDs	3.2	508	33	0.80
FTO/TiO$_2$/CdSe QDs/Au NPs	2.8	471	33	0.65

Figure 10. shows a schematic representation of the energy diagrams of the three photoanodes that employ Au NPs interfacial layer. The E$_{CB}$ of TiO$_2$ is -4.3 eV ,the work function (ϕ) of Au NPs is nearly -5.1 eV   which

lower than F_E of conducting FTO (-4.4 eV) (vacuum level) [16]. In configuration (i) as shown in Figure 10(a), the F_E of FTO can be modified to a lower energy due to the contact between Au NPs and FTO. The Au NPs work function create intermediate energy levels between TiO_2 and FTO/ Au NPs, that leads to easily transfer of electron from TiO_2 to FTO via Au NPs layer. Therefore, the presence of Au NPs layer on FTO enhances (J_{sc}) which is increased from 2.4 mA/cm^2 to 4.4 mA/cm^2. Also, this intermediate level is able to suppress the charge recombination through reducing back-transport reaction between the electrolyte and FTO layer which improve the V_{oc} from to 460 mV to 476 mV, and in turn the *PCE* is improved from 0.62% to 1.1% as could be seen in Table 3.
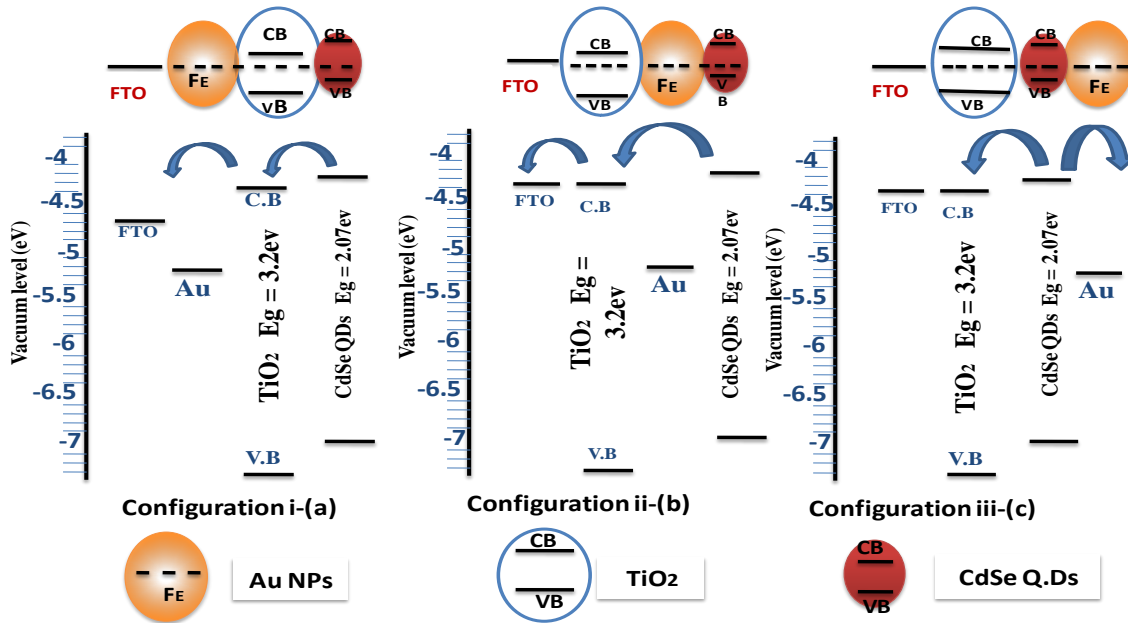

Figure 10: The energy diagram showing the alignment of the E_{vb} and E_{cb} of TBAI capped CdSe QDs and decorated with Au NPs on photoanodes for the three configuration (all data shown are vs. vacuum).

In configuration (ii), as shown in Figure 10(b), when Au NPs are deposited on TiO_2 this will create two Schottky barriers on the TiO_2 and CdSe QDs interfaces. This band bending creates an energy barrier, which promotes the photoexcited electrons in the Au NPs to be transferred effectively to the conduction band of the TiO_2, and a significant amount of the electrons generated in CdSe QDs and injected directly through the Au NPs will also reach the TiO_2 layer. The suggested design in configuration (ii) increases the J_{sc} is from 2.4 mA/cm^2 to 3.2 mA/cm^2 compared to the conventional design without Au NPs. Likewise V_{oc} which is controlled by the difference between the chemical potential of the polysulfide electrolyte and the CB of TiO_2, and is dependent on the external electric field created by the Au Plasmon field. The presence of the surface Plasmon modes provides a strong external electric field which enhances the V_{oc} from 460 mV to 508 mV.

In configuration (iii) as shown in Figure 10(c), Only CdSe QDs can be excited to generate electron - hole pairs. Since the Fermi level of Au NPs and the CB of TiO_2 are both lower than the CB of CdSe QDs, the photoelectrons created in the CdSe QDs will be capable to transfer along two ways; to the Au NPs and to the CB of TiO_2. A larger friction of electrons in the CB of CdSe QDs would flow into Au NPs more easily, because

Fermi level of Au NPs is lower than the CB of TiO$_2$, Meanwhile, a Schottky barrier at the interface of Au NPs-CdSe QDs will be formed, which can prevent the electrons to flow back to CdSe QDs from Au NPs. It is also reported that the electrons accumulated in the CB of TiO$_2$ may lead to a negative shift of the Fermi level. Therefore, fewer electrons accumulated in TiO$_2$, would result in a less negative shift of the Fermi level, leading to a slight increase in *Voc* from 460 mV to 471 mV [32]. The surface Plasmon electric field in Au NPs and the electron in the CB of CdSe QDs lead to a slight increase in *Jsc* from 2.4 mA/cm^2 to 2.8 mA/cm^2, so a slight increase in PCE from 0.62% to 0.65% as shown in Table 3.

4. Conclusions

The colloidal CdSe quantum dots (QDs) was synthesized using the organometallic method. A *PCE* of 0.62% was obtained from TBAI capped CdSe QDSSC that is much higher than 0.07% obtained from TOPO, HDA capped CdSe QDs device. The CdSe-QDSSCs modified with TBAI showed a large improvement photovoltaic performance and discussed in terms of atomic ligand and surface state of CdSe QDs. Au NPs with the average size of 15 nm was introduced to photoanodes QDSSCs via three configurations, on FTO substrate, in between TiO$_2$ NPs and CdSe QDs, and on the surface of CdSe QDs. The results show that the *PCE* by using Au NPs directly on the FTO substrate is 1.1% under one sun illumination, which is 60% higher than FTO/TiO$_2$/ CdSe QDs cell 0.62 % without Au NPs. From the investigation of energy level alignments for all configurations, the Fermi level F$_E$ of FTO could be modify to a lower energy by the contact between Au NPs and FTO which positively reflected on the QDSSC performance.

Acknowledgements

References

[1] Kamat, Prashant V. "Quantum dot solar cells. Semiconductor nanocrystals as light harvesters." The Journal of Physical Chemistry C" 112.48 (2008):18737-18753.

[2] Mehrabian, Masood, Kavoos Mirabbaszadeh, and Hossein Afarideh. "Experimental optimization of molar concentration to fabricate PbS quantum dots for solar cell applications. " Optik-International Journal for Light and Electron Optics 126, no. 5 (2015): 570-574.

[3] Kokate, Sunita K., Chaitali V. Jagtap, Prashant K. Baviskar, Sandesh R. Jadkar, Habib M. Pathan, and Kakasaheb C. Mohite. "CdS sensitized cadmium doped ZnO solar cell: Fabrication and characterizations." Optik-International Journal for Light and Electron Optics 157 (2018): 628-634.

[4] Tvrdy, Kevin, Pavel A. Frantsuzov, and Prashant V. Kamat. "Photoinduced electron transfer from semiconductor quantum dots to metal oxide nanoparticles. " Proceedings of the National Academy of Sciences" 108.1 (2011): 29-34

[5] Ali Badawi, N. Al-Hosiny, Amar Merazga, Ateyyah M. Albaradi, S. Abdallah, and H. Talaat. "Study of the back recombination processes of PbS quantum dots sensitized solar cells." Superlattices and Microstructures" 100 (2016): 694-702.

[6] Yang, Peizhi, Qunwei Tang, Chenming Ji, and Haobo Wang. "A strategy of combining SILAR with solvothermal process for In_2S_3 sensitized quantum dot-sensitized solar cells." Applied Surface Science" 357 (2015): 666-671.

[7] Singh, Neetu, R. M. Mehra, Avinashi Kapoor, and T. Soga. "ZnO based quantum dot sensitized solar cell using CdS quantum dots." Journal of renewable and sustainable energy"4, no. 1 (2012): 013110.

[8] Yum, Jun-Ho, Sang-Hyun Choi, Seok-Soon Kim, Dong-Yu Kim, and Yung-Eun Sung. "CdSe quantum dots sensitized TiO_2 electrodes for photovoltaic cells." Journal of the Korean Electrochemical Society" 10, no. 4 (2007): 257-261.

[9] Niu, Guangda, Liduo Wang, Rui Gao, Wenzhe Li, Xudong Guo, Haopeng Dong, and Yong Qiu. "Inorganic halogen ligands in quantum dots: I−, Br−, Cl− and film fabrication through electrophoretic deposition." Physical Chemistry Chemical Physics" 15, no. 45 (2013): 19595-19600.

[10] De La Fuente, Mauricio Solis, Rafael S. Sánchez, Victoria González-Pedro, Pablo P. Boix, S. G. Mhaisalkar, Marina E. Rincón, Juan Bisquert, and Iván Mora-Seró. "Effect of organic and inorganic passivation in quantum-dot-sensitized solar cells." The journal of physical chemistry letters" 4, no. 9 (2013): 1519-1525.

[11] Lu, Haipeng, Jimmy Joy, Rachel L. Gaspar, Stephen E. Bradforth, and Richard L. Brutchey. "Iodide-passivated colloidal PbS nanocrystals leading to highly efficient polymer: nanocrystal hybrid solar cells." Chemistry of Materials"28, no. 6 (2016): 1897-1906.

[12] Ayyaswamy, Arivarasan, Sasikala Ganapathy, Ali Alsalme, Abdulaziz Alghamdi, and Jayavel Ramasamy. "Structural, optical and photovoltaic properties of co-doped CdTe QDs for quantum dots sensitized solar cells." Superlattices and Microstructures" 88 (2015): 634-644

[13] Dao, Van-Duong, and Ho-Suk Choi. "Highly-efficient plasmon-enhanced dye-sensitized solar cells created by means of dry plasma reduction." Nanomaterials" 6, no. 4 (2016): 70

[14] Kouskoussa, B., M. Morsli, K. Benchouk, G. Louarn, Linda Cattin, A. Khelil, and J. C. Bernede. "On the improvement of the anode/organic material interface in organic solar cells by the presence of an ultra-thin gold layer." physica status solidi (a) " 206, no. 2 (2009): 311-315.

[15] Bernède, J. C., Y. Berredjem, L. Cattin, and M. Morsli. "Improvement of organic solar cell performances using a zinc oxide anode coated by an ultrathin metallic layer." Applied Physics Letters" 92, no. 8 (2008): 62   .

[16] Zhu, Guang, Fengfang Su, Tian Lv, Likun Pan, and Zhuo Sun. "Au nanoparticles as interfacial layer for CdS quantum dot-sensitized solar cells." Nanoscale research letters" 5, no. 11 (2010): 1749.

[17] Oliveira, Matheus Costa de, André Luis Silveira Fraga, Anderson Thesing, Rocelito Lopes de Andrade, Jacqueline Ferreira Leite Santos, and Marcos José Leite Santos. "Interface dependent plasmon induced enhancement in dye-sensitized solar cells using gold nanoparticles." Journal of Nanomaterials" 16, no. 1 (2015): 386.

[18] Zhong, Xinhua, Yaoyu Feng, and Yuliang Zhang. "Facile and reproducible synthesis of red-emitting CdSe nanocrystals in amine with long-term fixation of particle size and size distribution." The Journal of Physical Chemistry C" 111, no. 2 (2007): 526-531

[19] Zhu, Guang, Fengfang Su, Tian Lv, Likun Pan, and Zhuo Sun. "Au nanoparticles as interfacial layer for CdS quantum dot-sensitized solar cells." Nanoscale research letters" 5, no. 11 (2010): 1749

[20] Amr Hessein, Feijiu Wang, Hirokazu Masai, Kazunari Matsuda, and Ahmed Abd El-Moneim. "Improving the stability of CdS quantum dot sensitized solar cell using highly efficient and porous CuS counter electrode." Journal of Renewable and Sustainable Energy" 9, no. 2 (2017): 023504.

[21] Ha Thanh, Tung, Dat Huynh Thanh, and Vinh Quang Lam. "The CdS/CdSe/ZnS photoanode cosensitized solar cells basedon Pt, CuS, Cu_2S, and PbS counter electrodes." Advances in OptoElectronics" 2014 (2014).

[22] Yu, W. William, Lianhua Qu, Wenzhuo Guo, and Xiaogang Peng. "Experimental determination of the extinction coefficient of CdTe, CdSe, and CdS nanocrystals." Chemistry of Materials" 15, no. 14 (2003): 2854-2860.

[23] Kyobe, Joseph W., Egid B. Mubofu, Yahya MM Makame, Sixberth Mlowe, and Neerish Revaprasadu. "CdSe quantum dots capped with naturally occurring biobased oils." New Journal of Chemistry" 39, no. 9 (2015): 7251-7259.

[24] Thambidurai, M., N. Murugan, N. Muthukumarasamy, S. Vasantha, R. Balasundaraprabhu, and S. Agilan. "preparation and characterization of nanocrystalline CdS thin films.." Chalcogenide Letters" 6, no. 4 (2009).

[25] Madelung, Otfried. Semiconductors: data handbook. Springer Science & Business Media, 2012.

[26] Heba Hassan, T. Abdallah, S. Negm, and H. Talaat. "Rabi like angular splitting in Surface Plasmon Polariton–Exciton interaction in ATR configuration." Applied Surface Science" 441 (2018): 341-346.

[27] Truong, Nguyen Tam Nguyen, Woo Kyoung Kim, Umme Farva, Xiang Dong Luo, and Chinho Park. "Improvement of CdSe/P_3HT bulk hetero-junction solar cell performance due to ligand exchange from

TOPO to pyridine." Solar Energy Materials and Solar Cells" 95, no. 11 (2011): 3009-3014.

[28] Mohammed T.Hussein, Thekra K. Abd Al Raheem, Omar A. Ebrahim, Bushra A. Hassan, and Hasan B.J asim,'' Study the optical, structural and electrical properties of CdSe nanoparticles with different Se concentration. "International Journal of Engineering and Innovative Technology (IJEIT) ", 4, (2014) 2277.

[29] Hone, Fekadu Gashaw, Francis Kofi Ampong, Tizazu Abza, Isaac Nkrumah, Robert Kwame Nkum, and Francis Boakye. "Synthesis and characterization of CdSe nanocrystalline thin film by chemical bath deposition technique." Int. J. Thin. Fil. Sci. Tec" 4, no. 2 (2015): 69-74.

[30] Jasieniak, Jacek, Jessica Pacifico, Raffaella Signorini, Alessandro Chiasera, Maurizio Ferrari, Alessandro Martucci, and Paul Mulvaney. "Luminescence and Amplified Stimulated Emission in CdSe–ZnS-Nanocrystal-Doped TiO_2 and ZrO_2 Waveguides." Advanced Functional Materials" 17, no. 10 (2007): 1654-1662.

[31] Shao, Feiyan, Ming Li, Jianwen Yang, Yongpin Liu, and Lingzhi Zhang. "CdSe quantum dot-sensitized solar cell: Effect of size and attach mode of quantum dot." Journal of Nano Research" 30 (2015).

[32] Gao, Xin, Xiangxuan Liu, Zuoming Zhu, Ying Gao, Qingbo Wang, Fei Zhu, and Zheng Xie."Enhanced visible light photocatalytic performance of CdS sensitized TiO_2 nanorod arrays decorated with Au nanoparticles as electron sinks." Scientific reports" 7, no. 1 (2017): 973